# Preprints.org

Article

# Investigation of polyelectrolyte multilayers deposited on biodegradable corona charged substrates used as drug delivery systems

Asya Viraneva [*] , Maria Marudova , Sofia Milenkova , Aleksandar Grigorov , Temenuzhka Yovcheva

*Article*

# Investigation of Polyelectrolyte Multilayers Deposited on Biodegradable Corona Charged Substrates Used as Drug Delivery Systems

**Asya Viraneva \*, Maria Marudova, Sofia Milenkova, Aleksandar Grigorov and Temenuzhka Yovcheva**

University of Plovdiv "Paisii Hilendarski", 24 Tzar Assen str., Plovdiv, Bulgaria

\* Correspondence: asia83@abv.bg; Tel.: +359 32 261256

**Abstract:** Polyelectrolyte multilayers (PEMs) deposited on porous composite polylactic acid/poly(ε-caprolactone) substrates were studied. The substrates were previously charged in a corona discharge. Time dependences of the normalized surface potential for positively and negatively charged electrets were investigated. The morphology of the obtained porous substrates was examined by means of scanning electron microscopy (SEM). The chitosan and the casein polyelectrolytes were deposited on the substrates using the layer-by-layer (LbL) technique. A drug loading efficiency and the release kinetics were determined spectrophotometrically.

**Keywords:** porous composites; corona treatment; polyelectrolyte multilayers; drug delivery systems

## 1. Introduction

The rapid development of the polymer industry and the increasing demand for biodegradable alternatives of the most commonly used polymer products has led to more and more research being focused on the creation and characterization of such biodegradable and biocompatible products [1,2]. One major drawback of the implementation of most of the commonly used biopolymers is their poor mechanical properties, which in turn limits their wider applications. A common method for overcoming this drawback is the combination of different biopolymers with the aim of creating composite materials that possess more desirable properties, while maintaining most of the beneficial properties of each of the base polymer components. Composite biopolymers find applications in many fields, such as their biomedical application for the creation of drug carrying multilayers [3,4].

Amongst the most widely used biopolymers in the modern industry are poly-lactic acid (PLA), poly (ε-caprolactone) (PCL) and polyethylene glycol (PEG). These three biopolymers each possess desirable properties and can be used for a variety of products, however each of them also present a number of drawbacks that limits their wider applications.

Poly-lactic acid (PLA) is thermoplastic aliphatic polyester, that has become one of the most popular biopolymer for the synthesis of biodegradable products [5,6]. As a material PLA possesses a number of beneficial properties, such as good hydrophilicity, cell affinity and biodegradability. Additionally, PLA is often utilized as a base material for the creation of copolymers with a number of other biodegradable polymers.

Poly (ε-caprolactone) (PCL) is another biodegradable polymer that is often utilized for a number of biomedical and environmental applications. Due to its semicrystalline structure and lower degradation rate, when compared to PLA, poly (ε-caprolactone) is often used for the creation of long-term drug delivery applications and tissue engineering. However, its lack of chiral atoms makes it impossible to modify its properties by changing its stereochemistry, which limits its applicability [7]. For that reason, PCL is often copolymerized with PLA in order to tailor its properties [8].

With its high biocompatibility, polyethylene glycol (PEG) has found an increasing number of applications in the field of biomedicine [9]. The covalent grafting of PEG and its derivatives into

molecules has been shown to improve the biocompatibility and water solubility of said molecules, and is especially useful for the development of different drug delivery mechanisms [10]. PEG can also be used for surface modification, where it produces a biocompatible surface coating [11]. Additionally, PEG can also be used in combination with other polymers for the creation of composites with tailored properties [12].

Polymer blending is a proven and easy method of creation of composite structures with tailored properties. The most commonly used method for the creation of these composites is the copolymerization of two or more biopolymers, which yields a copolymer structure, whose properties can be adjusted by changing the ratio of each base polymer and their copolymerization conditions [13–15]. Another popular method for the creation of composite biopolymers is the use of different mechanical techniques, such as injection molding, extrusion or electrospinning [16–18]. All of those methods allow for the modification of the properties of the resulting composites to a certain degree. They can also be combined with different surface modification methods (such as plasma treatment) in order to further improve and modify their properties and create better biomaterials [19].

All of the described above methods aim to create a more biocompatible structure with desirable properties, which can later be used for numerous biomedical applications. One such application is controlled and targeted drug delivery with the use of biodegradable multilayers, created on the surface of the previously described composite biopolymers [20]. Often these multilayers are created with the use of a Layer-by-layer (LbL) deposition technique. This technique allows for the creation of thin multilayers with controlled properties, which can be loaded with a number of active biomolecules, such as different drugs [21], enzymes [22], nanoparticles, etc.

In our research paper we aim to investigate the influence of different ratios of the two chosen polymers (poly (D-lactic acid) and poly (ε-caprolactone)) on the drug loading and delivery properties of porous composite films.

## 2. Materials and Methods

### 2.1. Materials

Poly (ε-caprolactone) (PEC) was purchased from Lactel Absorbable Polymers (USA). Poly (D-lactic acid) (PDLA), polyethylene glycol (PEG), chitosan (high molecular mass, degree of deacetylation > 75%), sodium caseinate (casein sodium salt from bovine milk) and benzydamine hydrochloride were delivered from Sigma-Aldrich and were used without further purification. All other chemicals were with analytical grade.

### 2.2. Composite film creation

The porous composite films were created by first dissolving 4 % w/v PDLA and PEC in dichloromethane (DMC) on a magnetic stirrer at room temperature. Set amounts of the resulting solutions were then mixed to create three different PDLA/PEC mixtures with ratios 25/75, 50/50 and 75/25. Two additional pure solutions of PDLA and PEC were also prepared. Polyethylene glycol (PEG) was mixed into all five of the prepared solutions at a concentration of 150 % w/v and was stirred until a homogenous mixture was achieved. All solutions were then poured into glass plates, placed on a leveled surface and kept at a room temperature until the complete evaporation of the solvent. After that the resulting composite porous films were kept in an incubator for 24 hours at 35 ° C to ensure that any remaining moisture is removed from their surface.

### 2.3. Corona charging

The created porous composite films were cut into 2x2 cm samples and charged under corona discharge in normal atmospheric conditions. The setup used for the charging consisted of a needle electrode and a grounded plate, with a steel mesh placed between the two. For the charging process, 5 kV of set polarity was supplied to the needle electrode and 1 kV of the same polarity was supplied to the grid. This was done to ensure uniform distribution of the resulting charge on the surface of the

charged samples. All films were charged for 1 minute, with half of the samples being charged under positive corona and the other half under negative corona.

## 2.4. Surface charge distribution measurement

The surface charge potential of the charged samples was measured by the vibrating electrode method with compensation. This method consists of an electrode, placed above the charged surface, which is vibrated at a set frequency. The vibrating motion of the electrode within the electric field of the charged surface induces an alternating electric current within the electrode. This current can be compensated by applying an appropriate amount of outside voltage to the system, which cancels out the electric field of the sample and reduces the induced current to zero. By measuring the amount and polarity of the voltage, required for this compensation, one can determine the amount and polarity of the effective surface charge distribution, with the use of the following equation:

$$\sigma = (\varepsilon_0 \varepsilon / L) U_k, \tag{1}$$

Where $U_k$ is the compensation voltage, $\varepsilon$ is the relative dielectric permittivity of the sample, $\varepsilon_0$ is the dielectric permittivity of vacuum ($8{,}85 \times 10^{-12}$ F/m) and L is the sample thickness.

## 2.5. Layer-by-layer deposition

For the creation of the polyelectrolyte multilayers (PEMs), the prepared charged samples were attached on sample holders and placed in the deposition apparatus. Two different polyelectrolyte solutions were prepared for the dipping process: 300 ml of 0.1% w/v chitosan solution in acetate buffer (pH 5, 100 mM) and 300 ml 1% w/v casein solution in phosphate buffer (pH 8, 100 mM). The model drug Benzydamine Hydrochloride was dissolved in the chitosan solution at a concentration of 1g/ml. Deposition was carried out in a MSM SLEE Carousel Slide Stainer, using the following automated dipping program:

- Dipping in first polyelectrolyte solution for 15 minutes.
- Washing in deionized water for 5 minutes.
- Dipping in second polyelectrolyte solution for 15 minutes.
- Washing in deionized water for 5 minutes.

The order of the polyelectrolyte solutions was determined by the charge of the samples, with positive samples starting in the casein solution. The dipping process was carried out until the deposition of 4 bilayers on the surface of the sample.

## 2.6. Differential scanning calorimetry (DSC)

The phase state of the substrates was analyzed using the DSC 204F1 Phoenix instrument manufactured by Netzsch Gerätebau GmbH, Germany. Calibration of the instrument was carried out using an indium standard ($T_m$=156.6 °C, $\Delta H_m$=28.5 J/g) for both heat flow and temperature. Films were measured in hermetically sealed aluminum pans, with an empty pan serving as a reference. The measurements were conducted under an argon atmosphere, following the steps:

- Cooling down from 25 °C to -70 °C with cooling rate 2 K/min
- Isothermal step at -70 °C for 15 min
- Heating from -70 ° up to 300 ° with heating rate 10 K/min.

The melting temperature ($T_m$) and melting enthalpy ($\Delta H_m$) of the samples were determined using Netzsch Proteus – Thermal Analysis software. The percentage of crystallinity of PEC in the samples was calculated based on the determined melting enthalpy. Equation (2) was used for this calculation:

$$\chi_{PEC} = \frac{\Delta H_m}{\Delta H_m^0 \cdot \omega_{PEC}} \cdot 100 \tag{2}$$

where $\chi_{PEC}$ is the percentage of crystallinity of PEC; $\Delta H_m$ is the specific melting enthalpy [J.g$^{-1}$]; $\Delta H_m^0$ is the melting enthalpy of 100% crystalline polymer ($\Delta H_m^0 = 139.3$ J.g$^{-1}$ for PEC [23] and $\omega_{PEC}$ is the mass fraction of PEC.

The crystallinity of PDLA was determined from the melting enthalpy and cold crystallization enthalpy using equation (3):

$$\chi_{PDLA} = \frac{\Delta H_m}{\Delta H_m^0 \cdot \omega_{PDLA}} \cdot 100 \tag{3}$$

where $\chi_{PDLA}$ is the percentage of crystallinity of PDLA; $\Delta H_m$ is the melting enthalpy and of PDLA [J.g$^{-1}$]; $\Delta H_m^0$ is the melting enthalpy of 100% crystalline polymer ($\Delta H_m^0 = 106.0$ J.g$^{-1}$ [24] and $\omega_{PDLA}$ is the mass fraction of PDLA.

### 2.7. Scanning electron microscopy (SEM)

The examination of the morphology of the created PEMs was carried out with the use of scanning electron microscopy (SEM) (Prisma E SEM, Thermo Scientific, Waltham, MA, USA). Two milligrams of each of the tested samples were attached onto an aluminium holder and subsequently coated with carbon and gold, using a vacuum evaporator Quorum Q150T Plus (Quorum Technologies, West Sussex, UK). The resulting images were captured using a back-scattered electron detector (Prisma E SEM, Thermo Scientific, Waltham, MA, USA) at an accelerating voltage of 15 kV at different levels of magnification.

### 2.8. Water Contact angle Measurement

Water contact angle measurements were carried out under standard atmospheric conditions (at room temperature and normal air pressure). Five measurements for each type of modification were performed on different parts of the surface of the substrates. The collected measurements were averaged and used for the determination of the hydrophobicity of each type of samples. 2 µl droplets were used in order to decrease the impact of the surface roughness on the water contact angle measurements. The drops were carefully placed on the surface with the use of a 10 µl glass microsyringe (Innovative Labor System GmbH, Germany). The contact angles were determined by measuring the tangent of the drop profile from images, captured with a high resolution camera. The image processing was performed with the use of public domain ImageJ software (ImageJ v1.51k software).

### 2.9. Benzydamine hydrochloride (BH) drug release

Phosphate buffer saline (PBS) buffer with pH 7,4 and ionic strength of 100 mM was used for the determination of the drug release rate. Twenty milliliters of the buffer were placed in glass beakers and kept in a water bath at 37 ° C for the duration of the experiment. Three samples of each type of the multilayer films were placed in the beakers and stirred at 150 rpm for 8 hours. At set time intervals, 3 ml samples of the buffer were taken out and replaced with equal amounts of fresh buffer. The collected buffer samples were filtered through a 0.45 µm syringe filter and their absorption was measured at 306 nm with the use of a spectrophotometer. These results were used to for the determination of the time rate of the drug release.

### 2.10. Benzydamine hydrochloride (BH) drug content

Benzydamine hydrochloride loaded films were placed into 20 mL phosphate buffer saline (pH 7.4) and stirred continuously for 72 h on a magnetic stirrer. Then, the samples were sonicated for 5 minutes and filtered using ChromafilVR syringe filter (0.45 mm). Three samples of each type were measured during the test. The amount of BH was determined using UV/Vis spectrophotometer monitoring the band at a wavelength of 306 nm. The drug concentration was calculated from a standard calibration curve of BH in phosphate buffer saline (pH 7.4).

## 3. Results and discussion

### 3.1. Electret properties – time storage influence

The electret properties of the obtained porous composite substrates were investigated. Time dependences of the normalized surface potential for positively and negatively charged PDLA, PEC and PDLA/PEC electrets were studied for 6 hours. The surface potential was measured once every 5 minutes for the first 30 minutes, during which period the charge was rapidly decaying. After this, the surface potential was measured at longer intervals, due to the steady state values of the normalized surface potential stabilizing for all of the investigated electrets. The results for the steady state values of the surface potential for all investigated samples are presented in Figure 1.
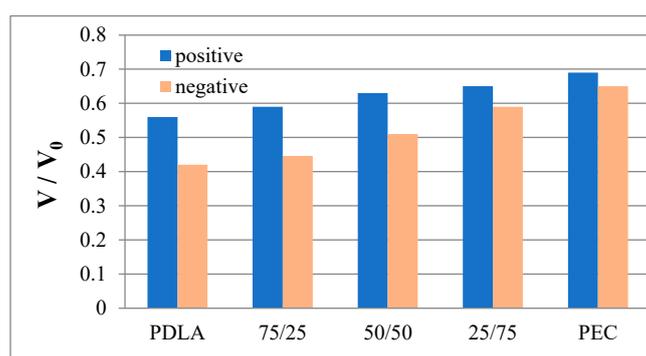


**Figure 1.** The steady state values of the normalized surface potential at the 6th hour for all investigated electrets.

The experimental results presented in Figure 1 demonstrate that the steady state values of the normalized surface potential for samples charged in a positive corona are higher than those charged in a negative corona for all investigated samples.

It was established in [25,26] that during the corona discharge in air, at atmospheric pressure, different types of ions are deposited on the sample, since the charging in a corona discharge depends on the corona polarity. In the case of a positive corona the ions are mainly $H^+(H_2O)n$ and the ones for a negative corona - $CO_3^-$. These ions are bound in traps of various depths and their release depends on the surrounding conditions.

It was also established, that the values of the normalized surface potential are the highest for pure PEC electrets and decrease when the content of PDLA increases. This is probably due to the very high degree of crystallinity, determined by the DSC method.

### 3.2. Phase state of polylactic acid / poly(ε-caprolactone) films

DSC analysis was conducted to ascertain the degrees of crystallinity in the examined samples. The heating curves obtained from this analysis are illustrated in Figure 2.
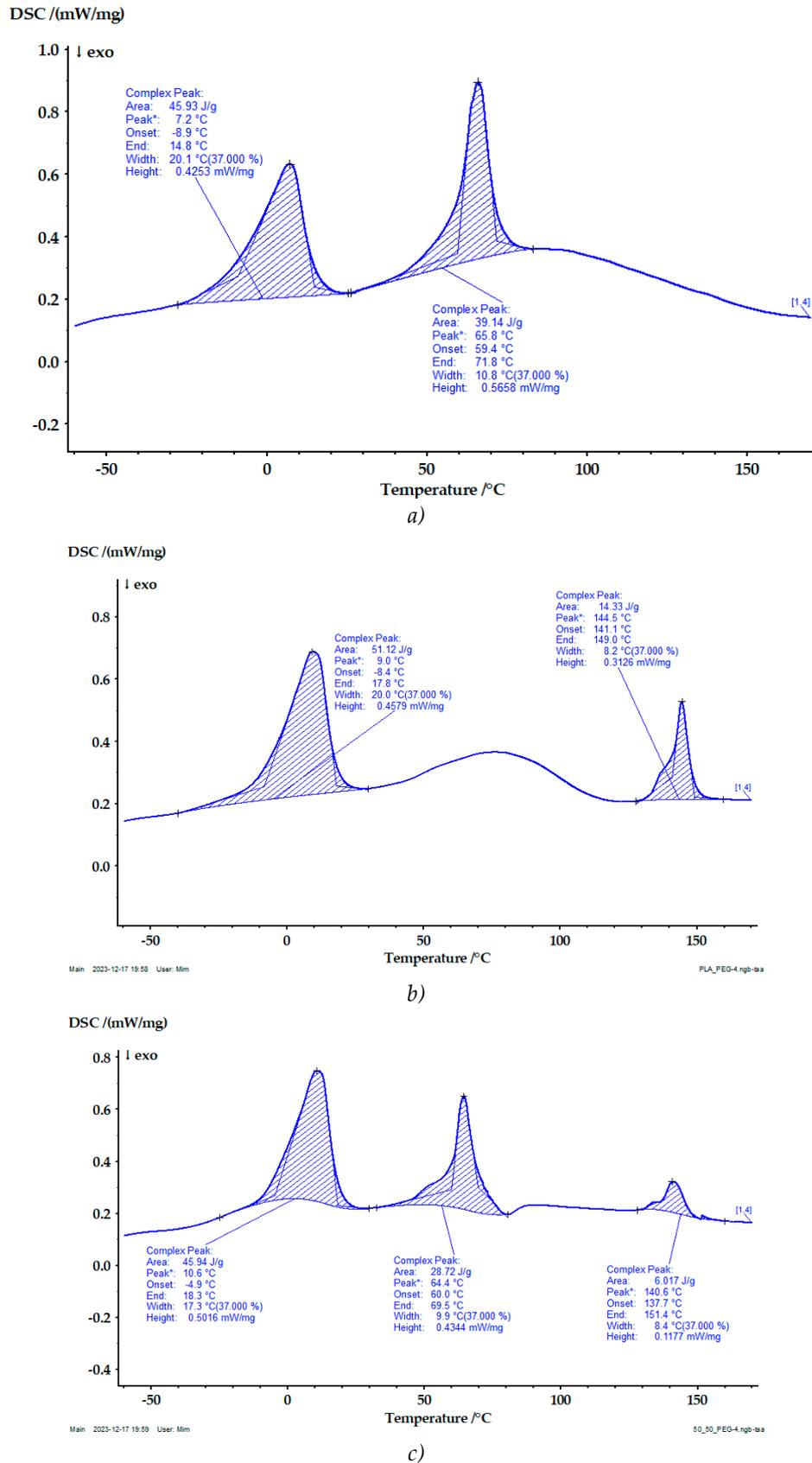
**Figure 2.** DSC curves of PDLA/PEC porous composite substrates: a)PEC; b)PDLA; c)50:50.

All thermograms clearly show the endothermic melting peak of polyethylene glycol, which occurs at a temperature of (7-10) °C. Its presence is proof of the presence of polyethylene glycol in the studied structures.

The glass transition temperature of PEC ($T_g \approx$ -63 °C) was not detected probably because of the very high degree of crystallinity.

The $T_g$ of PDLA was determined to be 50 °C, which is lower than cited in the literature [27]. This fact is probably due to the plasticizing effect of polyethylene glycol.

The melting phenomena of PEC is realized at lower temperature in comperison with a system without adding PEG. A possible reason could be an increase in the free volume in the polymer solution and the occurrence of additional interactions with the polyethylene glycol molecules that prevent the formation of larger and more stable crystallites.

The melting transitions in the PDLA/PEC blends were not affected by the blend composition, indicating their immiscibility at molecular level. Similar results are reported by other authors [28].

### 3.3. PEMs morphology

The PEMs morphology was investigated using Scanning electron microscopy (SEM). – Figure 3.
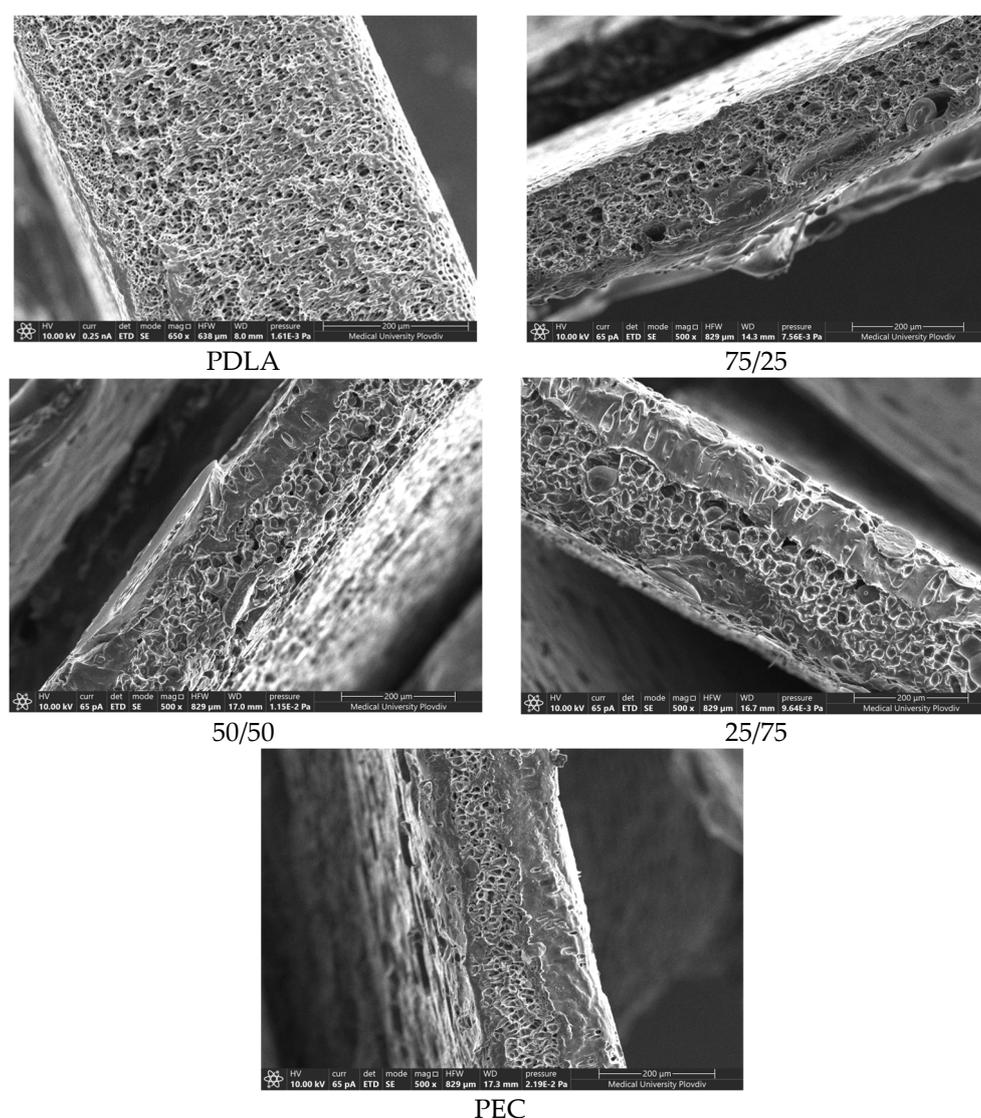


**Figure 3.** SEM images of PDLA/PEC porous composite substrates.

The pore sizes were calculated and the results are listed in Table 1. The presented values are average ones along with their standard deviations.

**Table 1.** Pore sizes based on measurement of randomly selected pores.

| Sample | Pore size diameter, μm |
|--------|------------------------|
| PDLA | 5.74 ± 1.42 |
| 75/25 | 18.76 ± 1.32 |
| 50/50 | 23.07 ± 1.87 |
| 25/75 | 24.59 ± 3.30 |
| PEC | 31.93 ± 2.87 |

The demand for the production of biocompatible porous materials in a single step process without harsh chemical modification continuously grows. Typical protocols of preparation are the salt leaching method, embedment of nano- or microparticles or usage of unfavorable types of solvents for the polymer [29–31]. A more suitable approach is the application of such types of liquid matterials, that will form stable solutions with minimal coalescence of drops to ensure homogenous pore formation. Since PEG 400 is both water-soluble and with low molecular weight, and exists in liquid form, it turns out to be a proper candidate for the preparation of microporous structures out of water insoluble polymers such as PDLA, PEC and their blends [32]. The results for the pore sizes for each 5 substrates are presented in Table 1. As it can be seen, pure PDLA substrate possess the smallest pore size diameter. Similar pore distribution and mean diameter were reported by Phaechamud and co-author [33]. Wang et al. (2019) suggest that the mechanism of void formation in PDLA is due to its plastic deformation in water conditions [34]. With the addition of PEC in sample 25:75, their size increased nearly 3 times. A trend of enlarging void diameters with the increase of the PEC concentration is observed and the largest pore diameter is reported for pure PEC samples. Same type of behavior reported Tsuji et al. (2006) [35]. Pore formation process is caused by the phase separation of the immiscible solvents, namely PEG 400 and chloroform and it takes place during the solvent evaporation phase. It was suggested that up to a certain polymer concentration, PDLA chains have better mobility, due to partial miscibility with PEG, leading to smaller voids. While in presence of PEC, PEG formed bigger particles, and subsequently pores, in the matrix, by diminishing the surface energy on the interface between them [36].

### 3.4. Water contact angle measurements

The wettability and the hydrophilicity of the investigated porous composite substrates was measured using static water contact angle method. The values of the water contact angle measurements obtained are presented in Figure 4.
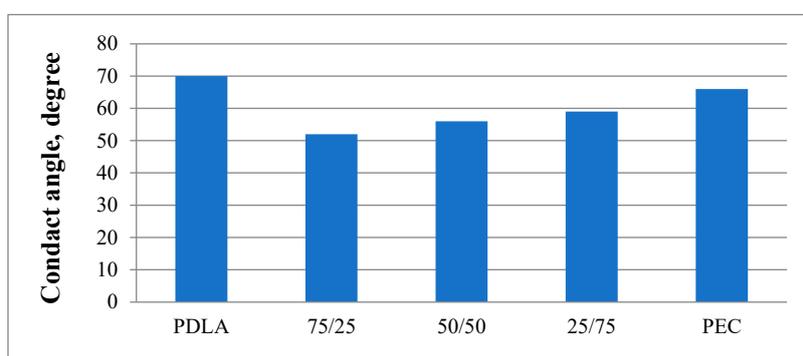


**Figure 4.** Water contact angle of all investigated samples.

The final value of the contact angle is the mean value of the 6 measurements. The estimated error was less than 5 %. The results presented in Figure 4 show that the PDLA had the largest contact angle (70°), indicating that it was the most hydrophobic material [37]. It was established that an increase in the surface wettability was observed with creating of composites. Upon addition of PEC into PDLA at different ratio, the contact angle decreased from 70° (pure PDLA) to 52° (75/25). A gradual increase

in the contact angle was observed with the increase of PEC content and reached 59° for 25/75 composites. This increase in the contact angle with increase of the PEC content is likely due to the increase of the pore sizes, shown in the surface morphology measurements (see SEM morphology) [38].

Following the theory of Owens and Wendt [39], the total surface free energy of all investigated samples was calculated. The results obtained are presented in Table 2.

**Table 2.** Surface free energy of all investigated samples.

| Sample | Surface energy, mJ/m$^2$ |
|--------|--------------------------|
| PDLA | 46.39 |
| 75/25 | 55.65 |
| 50/50 | 54.79 |
| 25/75 | 51.83 |
| PEC | 49.87 |

It was established that the surface free energy of PDLA/PEC composite substrates showed an increase when compared to the pure PDLA and PEC. The values of the surface free energy significantly increased for the modified films compared to base PDLA and PEC. In other words, the modified substrates were more hydrophilic than the original films [40].

### 3.5. Benzydamine hydrochloride (BH) drug content

Benzydamine hydrochloride was loaded in the chitosan/casein films deposited on composite substrates.

The drug amount, which was loaded to one PEM unit (2 x 2 cm) is presented in Figure 5.
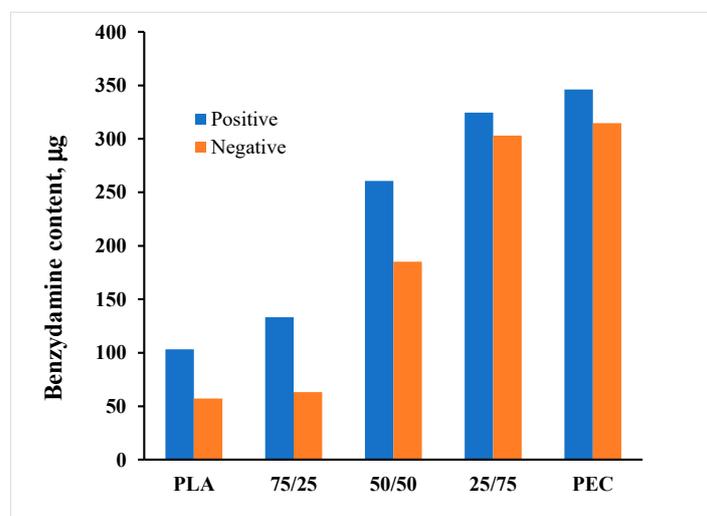


**Figure 5.** Benzydamine hydrochloride content in one PEM unit.

The data indicate a substantial impact of substrate composition on the loading efficiency of the PEMs. The quantity of loaded Benzydamine hydrochloride fluctuates between (50 ± 5) µg and (346 ± 0.3) µg, with an upward trend when PEC predominates in the substrate. The loading is most pronounced in PEMs constructed on PEC substrates. This observation aligns with the elevated values of the normalized surface potential of the PEC films, suggesting a potentially more stable structure for the PEMs under these conditions.

There is also a tendency for the amount of incorporated benzydamine to be greater in the structures deposited on positively charged substrates. Again, this dependence could be attributed to the more stable positive charge of the substrate.

*3.6. Benzydamine hydrochloride (BH) release*

The release kinetics of BH from PEMs assembled at different PDLA/PEC substrates is presented in Figure 6.
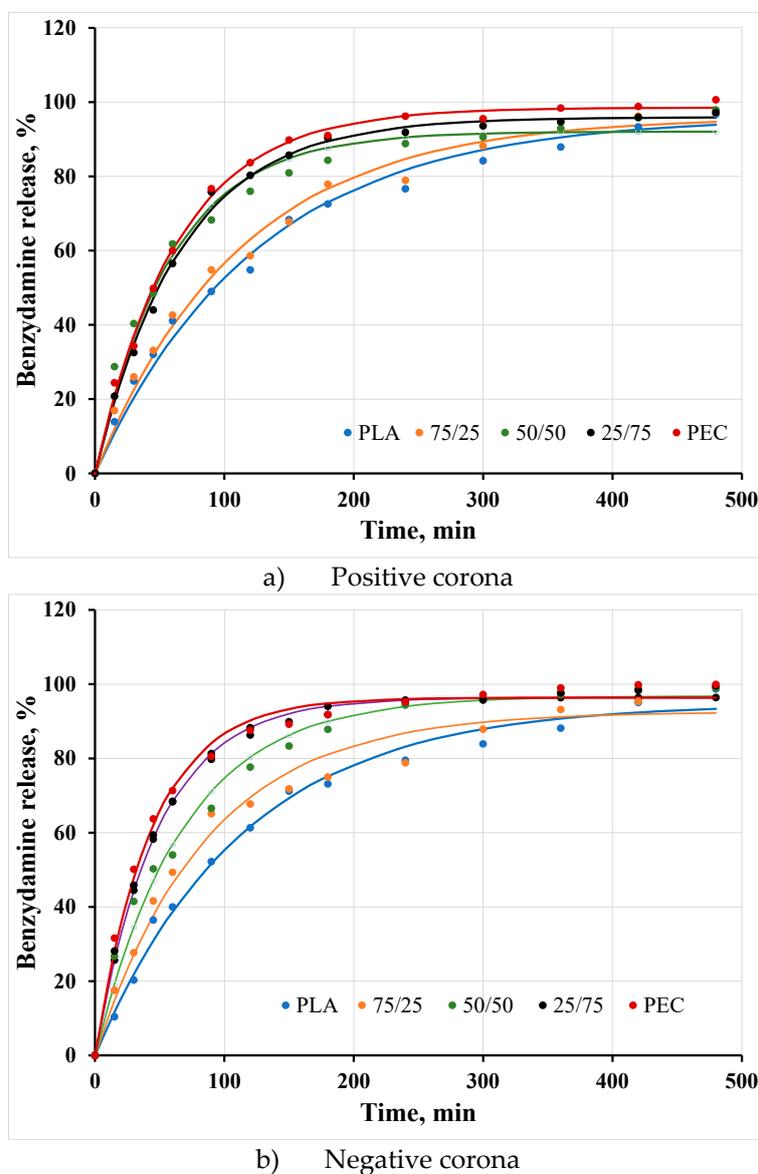


a)       Positive corona



b)       Negative corona

**Figure 6.** Benzydamine hydrochloride release from PEMs built-up on positive (a) and negative (b) corona charged substates.

The cumulative BH release was between 40 % – 75 % during the first hour and above 95 % during the first 8 hours. Therefore, it can be concluded that there is complete drug release within 8 hours.

The release kinetics greatly depend on the substrates composition. The observed results indicate the existence of a burst effect in case of of substrates with a predominant PEC content (neat PEC film and composite film 25:75), likely attributable to the porous nature of the films and a larger diffusion coefficient compared to structures without pores. Since the pores of PEC are larger, the tendency is the most pronounced. Benzydamine incorporated into polyelectrolyte structures built on PDLA-dominated substrates is fluent due to the smaller pore sizes and lower diffusion coefficient.

For better characterization of the release, the experimental results were subjected to mathematical processing according to the Weibull model (equation 4) [41]:

$$M = M_0 \left[ 1 - exp\left( -\frac{(t-T)}{\tau} \right)^{\beta} \right] \tag{4}$$

where $M$ is the amount of dissolved drug as a function of time; $M_0$ – the total amount of released drug; $t$ – time; $T$ – lag time caused by dissolution process; $\tau$ – scale parameter of the time dependence, and $\beta$ – shape of the dissolution curve progression. In our case "T" parameter is zero, because there is no lag time, and "$M_0$" parameter is 100 %.

The values of the Weibull model parameters for the measured release of BH are presented in Table 3.

**Table 3.** Weibull model parameters for BH release.

| Sample | Positive corona | | | Negative corona | | |
|--------|-----|-----|-----|-----|-----|-----|
| | $\tau$ | $\beta$ | $R^2$ | $\tau$ | $\beta$ | $R^2$ |
| PDLA | 153.1 | 1.10 | 0.991 | 163.4 | 1.42 | 0.991 |
| 75;25 | 120.3 | 1.07 | 0.998 | 150.1 | 1.74 | 0.979 |
| 50:50 | 99.1 | 1.08 | 0.981 | 89.5 | 1.32 | 0.986 |
| 25:75 | 68.95 | 1.03 | 0.996 | 66.0 | 1.37 | 0.996 |
| PEC | 68.0 | 1.07 | 0.997 | 57.2 | 1.32 | 0.991 |

The calculated values for $\tau$ exhibit an increase as the PDLA content in the substrates rises, indicating a prolonged release.

The value of $\beta$ for the positive corona charged substrate are close to 1, suggesting a combined release mechanism involving both Fick diffusion and swelling-controlled transport [42]. In this case the layers are tightly bount to the surface and do not dissolve.

For the negative corona charged samples, values of $\beta$ exceeding 1 signify a complex release mechanism: the release rate initially increases non-linearly up to the inflection point and then decreases asymptotically [43]. This behavior is indicative of drug molecules bound with varying degrees of tightness within the structure. A portion of the drug from the outer layers is released relatively easily and quickly, while the rest, bound more securely within the deeper layers, undergoes a slower and more challenging release, resulting in a decreased overall release rate.

Based on the results from the release kinetics, one may suggests that the drug release could be successfully controlled by changing the corona polarity and substrate content.

## 5. Conclusions

In this paper the BH release from PEMs, assembled on different porous composite PDLA / PEC substrates, was investigated. It was established that the steady state values of the normalized surface potential for PEC electrets are the highest compared to other investigated samples. This may be due to the highest value of the degree of crystallinity and the biggest pore sizes. The loading is most pronounced in PEMs constructed on PEC substrates. This observation aligns with the elevated values of the normalized surface potential of the PEC substrates, suggesting a potentially more stable structure for the PEMs under these conditions. The cumulative BH release was between 40 % – 75 % during the first hour and above 95 % during the first 8 hours. Therefore, it can be concluded that there is complete drug release within 8 hours.

## References

1.     Samir, A.; Ashour, F.H.; Hakim, A.A.A. et al. Recent advances in biodegradable polymers for sustainable applications. npj Mater Degrad 2022, 6, 68. https://doi.org/10.1038/s41529-022-00277-7

2.    Luckachan, G. E. & Pillai, C. K. S. Biodegradable Polymers - A Review on Recent Trends and Emerging Perspectives. J. of Polym. and the Env. 2011, 19(3), 637–676. doi:10.1007/s10924-011-0317-1

3.    Gopi, S.; Amalraj, A.; Sukumaran, N.P.; Haponiuk, J.T. and Thomas, S. Biopolymers and Their Composites for Drug Delivery: A Brief Review. Macromol. Symp. 2018, 380, 1800114. https://doi.org/10.1002/masy.201800114

4.    Cini, N. and Calisir, F. Layer-by-layer self-assembled emerging systems for nanosized drug delivery. Nanomed. 2022, 17:25, 1961-1980.

5.    Nath,P. C.; Nandi, N. B.; Tiwari, A.; Das, J.; Roy, B. In Nanotechnology Applications for Food Safety and Quality Monitoring, Sharma, A.; Vijayakumar, P.S.; Prabhakar, Er. P. K.; Kumar R.; Academic Press, 2023; Chapter 17 pp. 321-340. https://doi.org/10.1016/B978-0-323-85791-8.00006-9

6.    Cheng, Y.; Deng, S.; Chen, P. et al. Polylactic acid (PLA) synthesis and modifications: a review. Front. Chem. China 2009 4, 259–264. https://doi.org/10.1007/s11458-009-0092-x

7.    Coudane, J.; Nottelet, B.; Mouton, J.; Garric, X.; Van Den Berghe, H. Poly("-caprolactone)- Based Graft Copolymers: Synthesis Methods and Applications in the Biomedical Field: A Review. Molecules 2022, 27, 7339. https://doi.org/10.3390/molecules2721733939

8.    Cohn, D.; Hotovely Salomon, A. Designing biodegradable multiblock PCL/PLA thermoplastic elastomers. Biomaterials 2005, 26:15,, 2297-2305. https://doi.org/10.1016/j.biomaterials.2004.07.052

9.    D'souza A.A. & Shegokar R. Polyethylene glycol (PEG): a versatile polymer for pharmaceutical applications. Expert Opinion on Drug Delivery 2016, 13:9, 1257-1275. DOI: 10.1080/17425247.2016.1182485

10.   Hutanu et al. Recent Applications of Polyethylene Glycols (PEGs) and PEG Derivatives. Mod Chem appl 2014, 2:2

11.   Alcantar, N.A.; Aydil, E.S. and Israelachvili, J.N.  Polyethylene glycol–coated biocompatible surfaces. J. Biomed. Mater. Res. 2000, 51, 343-351. https://doi.org/10.1002/1097-4636(20000905)51:3<343::AID-JBM7>3.0.CO;2-D

12.   Ibrahim, M.;  Ramadan, E.; Elsadek, N.E.; Emam, S.E.; Shimizu, T.; Ando, H.; Ishima,  Y.; Elgarhy, O.M.; Sarhan, H.A.; Hussein, A.K. Ishida, T. Polyethylene glycol (PEG): The nature, immunogenicity, and role in the hypersensitivity of PEGylated products. J. of Contr. Rel. 2022, 351, 215-230. https://doi.org/10.1016/j.jconrel.2022.09.031

13.   Li, S.; Huang, M.H. Synthesis and characterization of block copolymers of e-caprolactone and DL-lactide initiated by ethylene glycol or poly(ethylene glycol). Macromol. Chem. and Phys. 2003, 204, 1994-2001. ⟨10.1002/macp.200350054⟩. ⟨hal-00418025⟩

14.   D'Antone, S.; Bignotti, F.; Sartore, L.; D'Amore, A.; Spagnoli, G.; Penco, M. Thermogravimetric investigation of two classes of block copolymers based on poly(lactic-glycolic acid) and poly(ε-caprolactone) or poly(ethylene glycol). Polym. Degrad. and Stab. 2001, 74:1, 119-124. https://doi.org/10.1016/S0141-3910(01)00110-0

15.   Matumba, K.I.; Motloung, M.P.; Ojijo, V.; Ray, S.S.; Sadiku, E.R. Investigation of the Effects of Chain Extender on Material Properties of PLA/PCL and PLA/PEG Blends: Comparative Study between Polycaprolactone and Polyethylene Glycol. Polymers 2023, 15, 2230. https://doi.org/10.3390/polym15092230

16.   Sharifisamani, E.; Mousazadegan, F.; Bagherzadeh, R.; Latifi, M. PEG-PLA-PCL based electrospun yarns with curcumin control release property as suture. Polym Eng Sci. 2020, 60, 1520–1529. https://doi.org/10.1002/pen.25398

17.   Douglas, P.; Albadarin, A.B.; Al-Muhtaseb, A.H. Mangwandi, C.; Walker, G.M. Thermo-mechanical properties of poly ε-caprolactone/poly l-lactic acid blends: Addition of nalidixic acid and polyethylene glycol additives. J. of the Mech. Beh. of Biomed. Mat. 2015, 45, 154-165. https://doi.org/10.1016/j.jmbbm.2015.01.022

18.   bdul Haq, R. H.; Marwah, O. M. F.; Abdol Rahman, M. N.; Ho, F. H.; Abdullah, H.; Ahmad, S., Tajul Arifin, A. M.; Hassan, M. F.; & Yunos, M. Z. Mechanical Properties of PCL/PLA/PEG composite blended with different molecular weight (MW) of PEG for Fused Deposition Modelling (FDM) filament wire. Intern. J. of Integr. Eng. 2018, 10(5).

19.   Hoque, M.; McDonagh, C.; Tiwari, B.K.; Kerry, J.P.; Pathania, S. Effect of Cold Plasma Treatment on the Packaging Properties of Biopolymer-Based Films: A Review. Appl. Sci. 2022, 12, 1346. https://doi.org/10.3390/app12031346

20.   Potaś, J.; Winnicka, K. The Potential of Polyelectrolyte Multilayer Films as Drug Delivery Materials. Int. J. Mol. Sci. 2022, 23, 3496. https://doi.org/10.3390/ijms23073496

21.   Bodurov I.; Marudova, M.; Viraneva, A.; T Yovcheva, T.; and Grigorov, A. Investigation of polyelectrolyte multilayers deposited on corona charged composite polylactic acid / poly(ε-caprolactone) substrates. J. Phys.: Conf. Ser. 2021, 1762, 012006. DOI 10.1088/1742-6596/1762/1/012006

22.   Grigorov, A.; Yovcheva, T.; Iliev, I.; Vlaeva, I.; Viraneva, A. Impact of physical and chemical modification on the immobilization of βgalactosidase in poly-lactic acid multilayer structures. Bulg. Chem. Comm. 2022, 54(B1), 47-52. DOI: 10.34049/bcc.54.B1.0389

23.   Chin-San, W. Physical Properties and Biodegradability of Maleated-Polycaprolactone/Starch Composite. Polym. Degrad. Stab. 2003, 80:1 , 127–134.

24.   Hutmacher, D.; Hürzeler, M.; Schliephake, H. A Review of Material Properties of Biodegradable and Bioresorbable Polymers and Devices for GTR and GBR Applications. Int. J. Oral Maxillofac. Implant. 1996 , 11, 667–678.

25.   Giacometti, J.; Fedosov, S.; and Costa, M. Corona charging of polymers: recent advances on constant current charging.   Brazilian J. Phys. 1999, 29:2, 269-279.

26.   Giacometti, J. A. and Oliveira, O. N. Corona charging of polymers. IEEE Trans. Electr. Insul. 1992, 27:5, 924-943.

27.   Baena, I.; Sessini, V.; Dominici, F.; Torre, L.; Kenny, J.; Peponi, L. Design of Biodegradable Blends Based on PLA and PCL: From Morphological, Thermal and Mechanical Studies to Shape Memory Behavior. Polym. Degrad. Stab. 2016, 132, 97–108.

28.   Priselac, D.; Poljaček, S.; Tomašegović, T.; Leskovac, M. Blends Based on Poly(ε-Caprolactone) with Addition of Poly(Lactic Acid) and Coconut Fibers: Thermal Analysis, Ageing Behavior and Application for Embossing Process. Polymers 2022, 14:9, 1792.

29.   Hossain, K. M. Z.; Felfel, R. M.; Ogbilikana, P. S.; Thakker, D.; Grant, D. M.; Scotchford, C. A.; & Ahmed, I. Single Solvent-Based Film Casting Method for the Production of Porous Polymer Films. Macromol. Mater. and Eng. 2018, 303(4), 1700628.

30.   Neri, F.; et.al. Biocompatible silver nanoparticles embedded in a PEG–PLA polymeric matrix for stimulated laser light drug release. J. of Nanop. Res. 2016, 18, 1-14.

31.   Park, S. B.; Sung, M. H.; Uyama, H.; & Han, D. K. Poly (glutamic acid): Production, composites, and medical applications of the next-generation biopolymer. Prog. in Pol. Sci. 2021, 113, 101341.

32.   Ma, Y.; Shi, F.; Wang, Z.; Wu, M.; Ma, J.; & Gao, C. Preparation and characterization of PSf/clay nanocomposite membranes with PEG 400 as a pore forming additive. Desalination 2012, 286, 131-137.

33.   Phaechamud, T.; & Chitrattha, S. Pore formation mechanism of porous poly (dl-lactic acid) matrix membrane. Mat. Sci. and Eng: C 2016, 61, 744-752.

34.   Wang, F.; Sun, Z.; Yin, J.; Xu, L. Preparation, Characterization and Properties of Porous PLA/PEG/Curcumin Composite Nanofibers for Antibacterial Application. Nanomaterials 2019, 9, 508.

35.   Tsuji, H.; & Horikawa, G. Porous biodegradable polyester blends of poly (L-lactic acid) and poly (ε-caprolactone): physical properties, morphology, and biodegradation. Polym. Internat. 2007, 56(2), 258-266.

36.   Lin, W. J.; & Lu, C. H. Characterization and permeation of microporous poly (ε-caprolactone) films. J. of Membr. Sci. 2002, 198(1), 109-118.

37.   Lu, Y.; Chen, Y.C.; Zhang, P.H. Preparation and Characterisation of Polylactic Acid (PLA)/Polycaprolactone (PCL) Composite Microfibre Membranes. FIBRES & TEXTILES in Eastern Europe 2016; 24, 3(117): 17-25.

38.   Alam, F.; Verma, P.; Mohammad, W.; Teo, J.; Varadarajan, K.M. and Kumar, S. Architected poly(lactic acid)/poly(e-caprolactone)/ halloysite nanotube composite scaffolds enabled by 3D printing for biomedical applications. J. Mater. Sci. 2021, 56, 14070-14083.

39.   Owens, D.K.; and Wendt R.C. Estimation of the surface free energy of polymers. J. Appl. Polym. Sci. 1969, 13:8, 1741-7.

40.   Khandwekar, A.; Patil, D.; Shouche, Y. and Doble, M. Surface Engineering of Polycaprolactone by Biomacromolecules and their Blood Compatibility. J. Biomat. Appl. 2011, 26, 227-252.

41.   Corsaro, C.; Neri, G.; Mezzasalma, A.M.; Fazio, E. Weibull Modeling of Controlled Drug Release from Ag-PMA Nanosystems. Polymers 2021 ,13:17 , 2897. doi: 10.3390/polym13172897. PMID: 34502937; PMCID: PMC8434431.

42.   Kobry´n, J.; Sowa, S.; Gasztych, M.; Dry´s, A.; and Musiał, W. Influence of Hydrophilic Polymers on the β Factor in Weibull Equation Applied to the Release Kinetics of a Biologically Active Complex of Aesculus hippocastanum. Intern. J. of Pol. Sci. 2017, 2017, 1-8.

43.   Papadopoulou, V.; Kosmidis, K.; Vlachou, M; and Macheras, P. On the use of the Weibull function for the discernment of drug release mechanisms. Intern. J. of Pharma. 2006, 309, 44–50.